Mecánica Computacional Vol. XXII
M. B. Rosales, V. H. Cortínez y D. V. Bambill (Editores)
Bahía Blanca, Argentina, Noviembre 2003

PARALLEL FINITE ELEMENT MODEL FOR COUPLED SURFACE AND SUBSURFACE FLOW IN HYDROLOGY: PROVINCE OF SANTA FE BASIN, ABSORBENT BOUNDARY CONDITION.

Rodrigo R. PAZ†, Mario A. STORTI†, Sergio R. IDELSOHN†, Leticia B. RODRIGUEZ‡ and Carlos A. VIONNET‡
†Centro Internacional de Métodos Computacionales en Ingeniería (CIMEC)
Universidad Nacional del Litoral, CONICET.
e-mail: rodrigop@intec.unl.edu.ar, url: http://www.cimec.org.ar
‡Grupo de Estudios Hidro-Ambientales (GEHA).
Universidad Nacional del Litoral, CONICET.
e-mail: vionnet@fich1.unl.edu.ar

Key Words: hydrology, surface and subsurface flow, absorbent boundary condition, finite element method, parallel computing.

Abstract. *The large spread in length scales present in the hydrological problems (i.e. province of Santa Fe basin systems) requires a high degree of refinement in the finite element mesh and, then, requires very large computational resources. Also, in a 2D multi-aquifer model, the number of unknowns per surface node is, at least, equal to the number of aquifers and aquitards. Moreover, if a pollutant transport model is used with the velocity field results, then it is desirable to have several sub-layers inside the aquifer in order to recover the vertical gradient, which drives the transport of pollutant between aquifers. This increases the number of unknowns and, also, the band-width of the associated FEM matrix, so that the total computation time is roughly proportional to the square of the number of vertical layers and sub-layers. Due to this fact, it is expected to have a very high demand of CPU computation time, calling for parallel processing techniques.*
A large scale C++ parallel FEM module using a general advection-diffusion PETSc-FEM code was written for hydrological problems. Several systems of aquifers/aquitards coupled with a net of surface streams can be solved. The streams can be modelled with the KWM (Kinematic Wave Model) approximation, 2D or 1D Saint-Venant model. There is mass exchange between streams and aquifers through a resistance coefficient at the stream walls. Both Manning and Chèzy friction models are available for the streams. Absorbent boundary conditions are implemented in order to avoid wave reflection for Saint-Venant models.

1 INTRODUCTION.

The aim of this work is to present the state of development of Large Scale Model for Surface and Subsurface water flow in multi-aquifer systems. The area under study is the argentinian Litoral, in the middle north-east of the country, where several non connected multi-aquifer/river systems are found (i.e Cululú, Las Conchas, San Antonio, Colastiné and Monjes-Cañada Carrizales drainage systems), (Fig. 1). This area represents 1/8 of the total area of the province of Santa Fe, Argentina. Therefore, the domain extension is about $16.000 Km^2$.

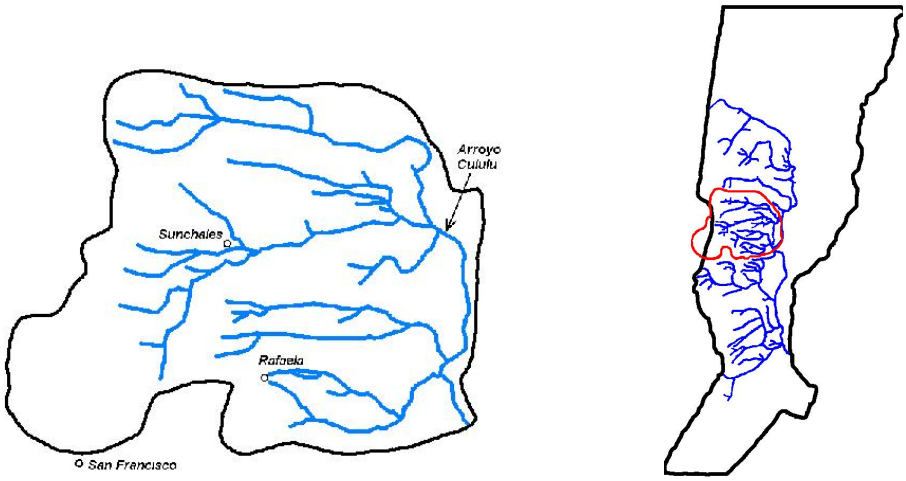

Figure 1: Drainage network and system location in province of Santa Fe.

Surface and subsurface water flow problems (i.e. multi-aquifer/river systems) deal with coupled nonlinear and linear differential equations in complex domains and dissimilar time scales. The problem is highly dependent on the terrain topology where water flows. We obtain the mesh and physical properties defined for the region via the Natural Neighbor interpolation from a Delaunay tesellation from satellite data images and the DTM data, digital terrain model (obtained from 88 topographical maps, scale 1:50.000).
The mathematical treatment of ground-water flows follows the confined aquifer theory or the classical Dupuit approximation for unconfined aquifers whereas surface-water flows are treated with the kinematic wave approximation or Saint-Venant model for open channel flow. A mathematical expression similar to Ohm's law is used to simulate the interacting term between the two hydrological components. The spread in time (slow time scale for ground-water flow and fast time scale for surface flow) and length scales requires an important degree of refinement in drainage network neighborhoods.

2 THE HYDROLOGICAL MODEL.

The implemented code solves the problem of subsurface flow in a free aquifer, coupled with a surface net of 2D or 1D streams (*"2D Saint-Venant Model"*, 2DSVM, *"1D Saint-*

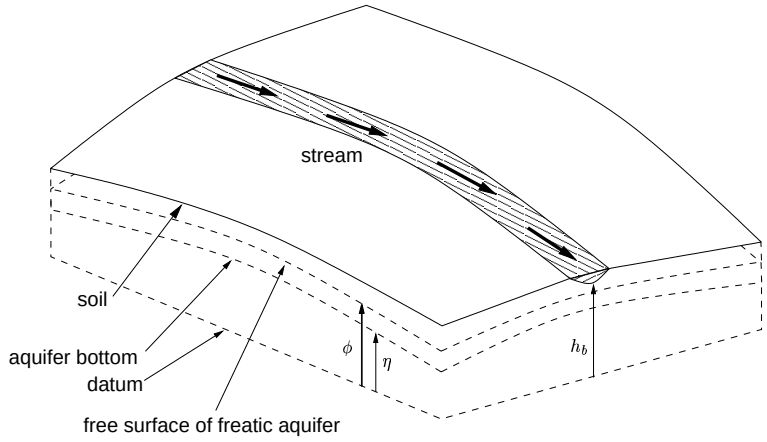

Figure 2: Aquifer/stream system.

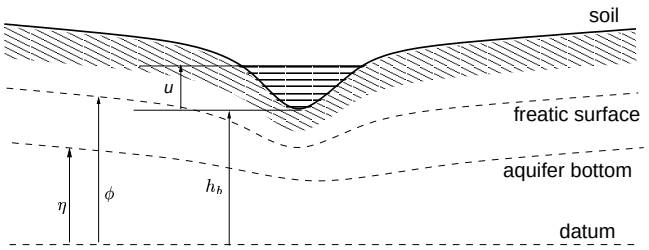

Figure 3: Aquifer/stream system. Transverse 2D view.

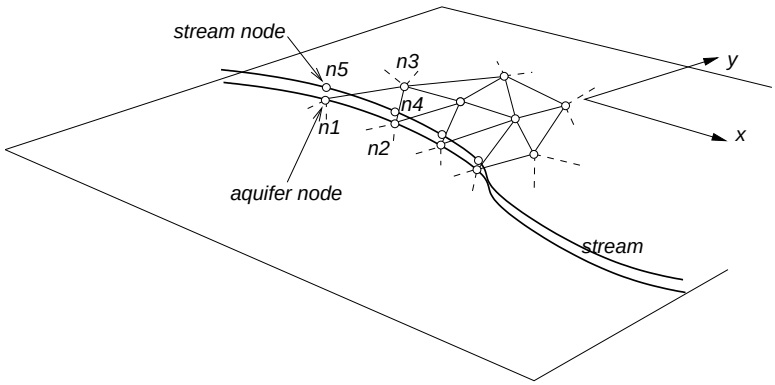

Figure 4: Aquifer/stream discrete system.

Venant Model", 1DSVM, and *"Kinematic Wave model"*, KWM). To model such system three element sets must be used: an *aquifer* system representing the subsurface aquifer, a 2D or 1D (depending on the chosen model) *stream* element set representing the stream and a 2D or 1D *stream loss* element set representing the losses from the stream to the aquifer (or vice versa) see Fig. 2 and Fig. 3.

2.1 Subsurface Flow.

The *aquifer* element set is 2D linear triangle or quadrangle elements (see Fig. 4). A per-node property η represents the height of the aquifer bottom to a given datum. The corresponding unknown for each node is the piezometric height or the level of the freatic surface at that point ϕ.
The equation for the aquifer integrated in the vertical direction is

$$\frac{\partial}{\partial t}\left(S(\phi-\eta)\phi\right) = \nabla\cdot\left(K(\phi-\eta)\nabla\phi\right) + \sum G_a, \quad \text{on } \Omega_{aq}\times(0,t], \tag{1}$$

where Ω_{aq} is the aquifer domain, S is the storativity, K is the hydraulic conductivity and G_a is a source term, due to rain, losses from streams or other aquifers.

2.2 Surface Flow.

2.2.1 2D Saint-Venant Model.

The *stream* element set represents a 2D or 1D stream of water. It has its own nodes, separated from the aquifer nodes, whose coordinates must coincide with some corresponding node in the aquifer. A constant per node field represents the stream bottom height h_b, with reference to the datum. That is why, normally, we have two coordinates and the stream bottom height for each node.
The equations for the 2D Saint-Venant open channel flow are the well known mass and momentum conservation equations integrated in the vertical direction. If we write this equations in the conservation matrix form, we have

$$\frac{\partial \mathbf{U}}{\partial t} + \frac{\partial \mathbf{F}_i(\mathbf{U})}{\partial x_i} = \mathbf{G}_i(\mathbf{U}), \qquad i=1,..,3, \quad \text{on } \Omega_{st}\times(0,t], \tag{2}$$

where Ω_{st} is the stream domain, $\mathbf{U} = (h, hw, hv)^T$ is the state vector and the advective flux functions in Eq. 2 are

$$\begin{aligned} \mathbf{F}_1(\mathbf{U}) &= (hw, hw^2 + g\frac{h^2}{2}, hwv)^T, \\ \mathbf{F}_2(\mathbf{U}) &= (hv, hwv, hv^2 + g\frac{h^2}{2})^T, \end{aligned} \tag{3}$$

where h is the height of the water in the channel with respect to the channel bottom, $\mathbf{u} = (w, v)^T$ is the velocity vector and g is the acceleration due to gravity. As in Eq. 1,

G_s represents the gain (or loss) of the river, the source term is

$$\mathbf{G}(\mathbf{U}) = (G_s,\ gh(S_{0x} - S_{fx}) + f_c hv + C_f \varpi_x |\varpi|,\ gh(S_{0y} - S_{fy}) - f_c hw + C_f \varpi_y |\varpi|)^T \quad (4)$$

where S_0 is the bottom slope and S_f is the slope friction.

$$\begin{aligned} S_{fx} &= \frac{1}{C_h h} w|\bar{u}|, \quad S_{fy} = \frac{1}{C_h h} v|\bar{u}| \quad \text{Chèzy model.} \\ S_{fx} &= \frac{n^2}{h^{4/3}} w|\bar{u}|, \quad S_{fy} = \frac{n^2}{h^{4/3}} v|\bar{u}|, \quad \text{Manning model.} \end{aligned} \quad (5)$$

where C_h and n (the Manning roughness) are model constants. Generally, the effect of coriolis force, related to the coriolis factor f_c, must be taken in account in the case of great lakes, wide rivers and estuaries. The coriolis factor is given by $f_c = 2\omega \sin\psi$, where ω is the rotational rate of the earth and ψ is the latitude of the area under study. The free surface stresses in Eq. 4 are expressed as the product between a friction coefficient and a quadratic form of the wind velocity, $\varpi(\varpi_x, \varpi_y)$, and

$$C_f = c_\varpi \frac{\rho_{air}}{\rho}, \quad (6)$$

where,

$$\begin{aligned} c_\varpi &= 1.25 \times 10^{-3} \varpi^{-1/5} \quad \text{if } |\varpi| < 1 \text{ m/s}, \\ c_\varpi &= 0.5 \times 10^{-3} \varpi^{1/2} \quad \text{if } 1 \text{ m/s} \leq |\varpi| < 15 \text{ m/s}, \\ c_\varpi &= 2.6 \times 10^{-3} \quad \text{if } |\varpi| \geq 15 \text{ m/s}, \end{aligned} \quad (7)$$

2.2.2 1D Saint-Venant Model.

When velocity variations on the channel cross section are neglected, the flow can be treated as one dimensional. The equations of mass and momentum conservation on a variable cross sectional stream (in conservation form) are,

$$\begin{aligned} \frac{\partial \mathbf{A}(s,t)}{\partial t} + \frac{\partial \mathbf{Q}(\mathbf{A}(s,t))}{\partial s} &= G_s(s,t), \\ \frac{1}{\mathbf{A}(s,t)} \frac{\partial \mathbf{Q}}{\partial t} + \frac{1}{\mathbf{A}(s,t)} \frac{\partial}{\partial s} (\beta \frac{\mathbf{Q}^2}{\mathbf{A}(s,t)}) + g(S_0 - S_f) + & \\ + g\frac{\partial h}{\partial s} - \frac{c_\varpi}{\mathbf{A}(s,t)} \varpi^2 cos\alpha &= \frac{q_t}{\mathbf{A}(s,t)} (v - v_t), \quad \text{on } \Omega_{st} \times (0,t], \end{aligned} \quad (8)$$

where $\mathbf{A}$ is the cross sectional area, $\mathbf{Q}$ is the discharge, $G_s(s,t)$ represents the gain or loss of the stream (i.e. the lateral inflow per unit length of channel), s is the arc-length along the channel, $v = \mathbf{Q}/\mathbf{A}$ the average velocity in s-direction, v_t the velocity component

in s-direction of lateral flow from tributaries, the Boussinesq coefficient $\beta = \frac{1}{v^2 \mathbf{A}} \int u^2 dA$ (u the flow velocity at a point) and α the wind direction measured from a positive line tangent to s in flow direction. The bottom shear stresses are approximated by using the Chèzy or Manning equations,

$$\begin{aligned} S_f &= \frac{v^2}{C_h^2} \frac{P(h)}{\mathbf{A}(h)}, \quad \text{Chèzy model.} \\ S_f &= \left(\frac{n}{a}\right)^2 v^2 \frac{P^{4/3}(h)}{\mathbf{A}^{4/3}(h)}, \quad \text{Manning model.} \end{aligned} \tag{9}$$

where P is the wetted perimeter of the channel and a is a conversion factor ($a = 1$ for metric units).

2.2.3 Kinematic Wave Model.[1]

When friction and gravity effects dominate over inertia and pressure forces, and, if we neglect the stress due to wind blowing and the coriolis term, the momentum equation becomes

$$S = S_f, \tag{10}$$

and Eq. 8

$$\frac{\partial \mathbf{A}(h)}{\partial t} + \frac{\partial \mathbf{Q}(\mathbf{A}(h))}{\partial s} = G_s, \quad \text{on } \Omega_{st} \times (0, t], \tag{11}$$

where $\mathbf{A}$ depends, through the geometry of the channel, on the channel water height h. The flow rate $\mathbf{Q}$ under the KWM model is only a function of $\mathbf{A}$ through the friction law.

$$\mathbf{Q} = \gamma \mathbf{A}^m, \tag{12}$$

where $\gamma = C_h\, S^{1/2}\, P^{-1}$ and $m = 3/2$ for the Chèzy friction model, and $\gamma = \bar{a}\, n^{-1}\, S^{1/2}\, P^{-2/3}$ and $m = 5/3$ for the Manning model; $S = (\mathrm{d}h_b/\mathrm{d}s)$ is the slope of the stream bottom.

2.3 Boundary Conditions.

2.3.1 Boundary Conditions to simulate River-Aquifer Interactions/Coupling Term.

The stream/aquifer interaction process occurs between a stream and its adjacent flood-plain aquifer. The coupling term is not explicitly included in Eq. 1 but it is treated as a boundary flux integral. At a nodal point we can write the coupling,

$$G_s = P/R_f(\phi - h_b - h), \tag{13}$$

where G_s represents the gain or loss of the stream, and the main component is the loss to the aquifer and R_f is the resistivity factor per unit arc length of the perimeter. The corresponding gain to the aquifer is

$$G_a = -G_s\, \delta_{\Gamma_s}, \tag{14}$$

where Γ_s represents the planar curve of the stream and δ_{Γ_s} is a Dirac's delta distribution with a unit intensity per unit length, i.e.

$$\int f(\mathbf{x})\,\delta_{\Gamma_s}\,\mathrm{d}\Sigma = \int_0^L f(\mathbf{x}(s))\,\mathrm{d}s. \tag{15}$$

The *stream loss* element set represents this loss, and a typical discretization is shown in Fig. 4. The stream loss element is connected to two nodes on the stream and two on the aquifer. If the stream level is over the freatic aquifer level ($h_b + h > \phi$) then the stream losses water to the aquifer and vice versa. Contrary to standard approaches, the coupling term is incorporated through a boundary flux integral that arises naturally in the weak form of the governing equations rather than through a source term.

2.3.2 Initial Conditions. First, Second and Third Kind Boundary Conditions/Absorbent Boundary Condition.

Groundwater flow. In the previous section, the equation that governs subsurface flow was established. In order to obtain a well posed PDE problem, initial and boundary conditions must be superimposed on the flow domain and on its limits. The initial condition for the groundwater problem is a constant hydraulic head in the whole region that obeys levels observed in the basin history.
Now, consider a simply connected region Ω bounded by a closed curve $\partial\Omega$ such that $\partial\Omega_\phi \cup \partial\Omega_\sigma \cup \partial\Omega_{\phi\sigma} = \partial\Omega$. If the stream is partially penetrating and connected, in a Hydraulic sense, to the aquifer, we set

$$\begin{aligned} \phi &= \phi_0, \quad \text{on } \partial\Omega_\phi \times (0,t] \\ K(\phi-\eta)\frac{\partial\phi}{\partial n} &= \sigma_0, \quad \text{on } \partial\Omega_\sigma \times (0,t] \\ K(\phi-\eta)\frac{\partial\phi}{\partial n} &= C(\phi-h), \quad \text{on } \partial\Omega_{\phi\sigma} \times (0,t] \end{aligned} \tag{16}$$

where ϕ_0 is a given water head, σ_0 is a given flux normal to the flux boundary $\partial\Omega_\sigma$ and C the conductance at the river/stream interface. If a fully penetrating stream is considered,

$$K(\phi-\eta)\frac{\partial\phi}{\partial n} = C(\phi-h), \quad \text{on } \partial\Omega_{\phi\sigma} \times (0,t] \tag{17}$$

Finally, for a perched stream,

$$K(\phi-\eta)\frac{\partial\phi}{\partial n} = C(h_b-h), \quad \text{on } \partial\Omega_{\phi\sigma} \times (0,t] \tag{18}$$

Surface Flow - Fluid Boundary. We recall that the type of a flow in a stream or in an open channel depends on the value of the Froud number $F_r = |\mathbf{u}|/c$ (where $c = \sqrt{gh}$ is the wave celerity), a flow is said

- fluvial, for $|\mathbf{u}| < c$.
- torrential, for $|\mathbf{u}| > c$

Saint-Venant equations. Considering a *Cauchy* problem for the time-like variable $x^{dim+1} = t$ where the solution is given in the subspace $x^{dim+1} = t = 0$ as $\mathbf{U} = \mathbf{U}(\mathbf{x}, t = 0)$ and is determined at subsequent values of t. If the subspace $t = 0$ is bounded by a surface $\partial\Gamma(\mathbf{x})$ then additional conditions have to be imposed on that surface at all values of t. This defines an *initial boundary value problem*. A solution for the system of the first-order PDE's can be written as a superposition of wave-like solutions of the type corresponding to the n-eigenvalues of the matrix $\mathbf{A}^k \cdot \mathbf{n} = \frac{\partial \mathbf{F}_i(\mathbf{U})}{\partial \mathbf{U}}^k \cdot \mathbf{n}, \qquad k = 1, .., dim$, being $\mathbf{n}$ the outward unit normal to the boundary edge:

$$\mathbf{U} = \sum_{\alpha=1}^{n} \bar{\mathbf{U}}_\alpha e^{\mathbf{I}(\mathbf{x}\cdot\mathbf{n} - \omega_\alpha t)}, \quad \text{on } \Omega_{st} \times \Gamma_{st} \times (0, t] \tag{19}$$

where summation extends over all eigenvalues λ_α.
As the problem is hyperbolic, n initial conditions for the *Cauchy* problem have to be given to determine the solution. That is, equal number of conditions as unknowns must be imposed at $t = 0$. For initial boundary value problem the n boundary conditions have to be distributed along the limits at all values of t, according to the direction of the propagation of the corresponding waves. If the wave phase velocity, the α-eigenvalue of $\mathbf{A}^k \cdot \mathbf{n}_k$ (i.e. k-wave projected in the interior normal direction $\mathbf{n}$), is positive, the information is propagated inside the domain. Hence, the number of conditions to be imposed for the initial boundary value problem at a given point of $\partial\Gamma$ is equal to the number of positive eigenvalues of $\mathbf{A}^k \cdot \mathbf{n}_k$ at that point. The total number of conditions remains equal to the total number of eigenvalues (i.e. the order of the system). For the treatment of the boundary conditions we will use the one dimensional projected system and consider the sign of the eigenvalues of $\mathbf{A}^k$ ($u_n + c$ and $u_n - c$). We remark that if $\mathbf{n}$ is the outward unit normal to the boundary edge, an inflow boundary corresponds to $\mathbf{u} \cdot \mathbf{n} < 0$ and an outflow one to $\mathbf{u} \cdot \mathbf{n} > 0$.

Fluvial Boundary.

- inflow boundary: $\mathbf{u}$ specified and the depth h is extrapolated from interior points, or vice versa.
- outflow boundary: depth h specified and velocity field extrapolated from interior points, or vice versa.

Torrential Boundary.

- inflow boundary: $\mathbf{u}$ and the depth h are specified.
- outflow boundary: all variables are extrapolated from interior points.

Solid Wall Condition. We prescribe the simple slip condition over Γ_{slip} ($\subset \Gamma_{st}$)

$$\mathbf{u} \cdot \mathbf{n} = 0 \tag{20}$$

Kinematic Wave Model. The applicability of the kinematic wave as an approximation to dynamic wave was discussed in *Rodríguez*[1](1995) and, according to Lighthill and Whitham, subcritical flow conditions favor the kinematic approach.
Since one characteristic is propagated inside the domain, only we can specify the water head, the channel section or the discharge at inflow boundaries (see Eq. 12).

Absorbent Boundary Condition. In order to avoid wave reflections in fictitious boundaries (computational boundaries) we present an scheme based on an *extrapolation method* using *Lagrange multipliers* as nonlinear restrictions. For simplicity reasons we develop the unidimensional case. The extrapolation to a multi-dimensional case is straightforward. The basic idea is to fix the characteristic variables, or equivalently, the Riemann Invariants at nodes in Γ_{stream} to a reference state, the absorbent condition or any characteristic variable state, via the superimposition of nonlinear restrictions with Lagrange Multipliers.
As it was already stated, the number of boundary conditions to be imposed will depend on the way the information transported along the characteristics interacts with the boundaries (see Fig. 5). At an inflow point N_0 the characteristic C^+ has a slope $u + c$, which is always positive for a flow in the $\mathbf{x}$ positive direction. Therefore, it will always carry information from the boundaries towards the inside of the domain. The second characteristic C^- has a slope whose sign depends on the inflow *froude* number. For torrential inflow, C^- will have a positive slope, but a negative slope at a fluvial inflow condition. In the first case, the information from the inflow surface enters the domain and a corresponding boundary condition has to be imposed. In the other hand, at a fluvial inflow, information from inside the domain reaches the boundary along C^- and no boundary condition associated with C^- is allowed to be fixed arbitrarily. Similar considerations can be made at an outflow border. The characteristic C^+ always reaches the outflow border from inside the domain and therefore it determines the other independent characteristic variable in the outflow plane from the behavior of the interior flow. Then, the *extrapolation* conditions for the fluvial regime are:

- at inflow boundaries,

$$\begin{aligned} R_0^+ &= R_1^+, \\ R_0^- &= R_{ref\_\,in}^-, \end{aligned} \tag{21}$$

- at outflow boundaries,

$$\begin{aligned} R_N^+ &= R_{N-1}^+, \\ R_N^- &= R_{ref\_\,out}^-, \end{aligned} \tag{22}$$

where $R^+ = \mathbf{u} \cdot \mathbf{n} + 2c$ and $R^- = \mathbf{u} \cdot \mathbf{n} - 2c$ are the Riemann Invariants (correspondent to C^+ and C^- characteristics respectively) projected in the outside surface normal direction, and the subscripts refer to the point where the invariants are calculated (see Fig. 6).
The absorbent element set implemented has three nodes: the boundary node, one neighboring inner node to the boundary node and a *"dummy"* node that gives the necessary d.o.f's for Lagrange Multipliers.
Using Lagrange multipliers leads to diagonal null terms, which can cause zero pivots when using direct methods. Therefore, a small term is added to the diagonal in order to fix the zero pivots. The term is added in the Jacobian or also in the residual (the results would be non-consistent). A diagonal term, proportional to the small term, may be also entered in the residual. If this is term is 1, then the method is "non-consistent", i.e. the restriction is not exactly satisfied by the non-linear scheme (Newton-Raphson). If the term is 0 then the restriction is consistently satisfied but with a non exact Newton-Raphson. Also, we can scale the columns in the matrix that correspond to the Lagrange Multipliers by a factor which can help a well system condition. Finally, we remark that the residuals and jacobians are calculated implicitly.

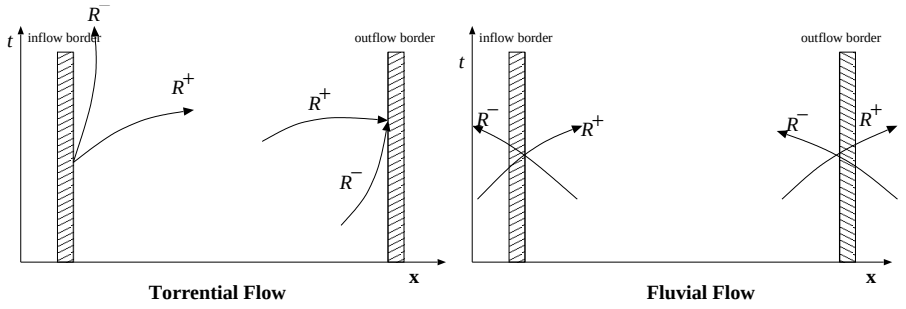

Figure 5: Inflow/Outflow Characteristics.

3 NATURAL NEIGHBOR INTERPOLATION.[2]

In order to interpolate physical properties and topographical data from DTM maps we have implemented the Natural Neighbor interpolation function using CGAL geometrical library[3](http://www.cgal.com/). Natural Neighbor shape functions are C^∞ everywhere, except at the support nodes where they are C^0. This and other properties[4] make them powerful in order to obtain smooth interpolations. For instance, we can see in Fig. 7 the height interpolation for nodal point of a refined triangulation for our stream/aquifer FEM application (in black) from iso-height data points DTM map (height-colored surface) using the natural neighbor algorithm proposed in Paz *et al.*(2002)

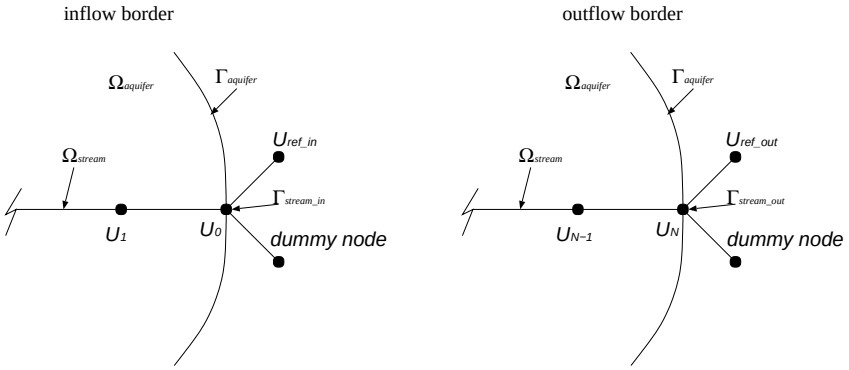

Figure 6: Absorbent Element.

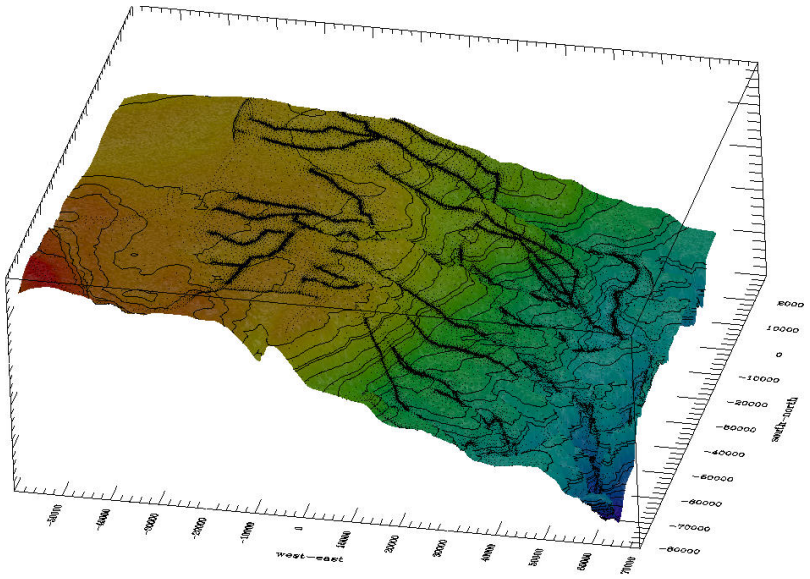

Figure 7: Height interpolation.

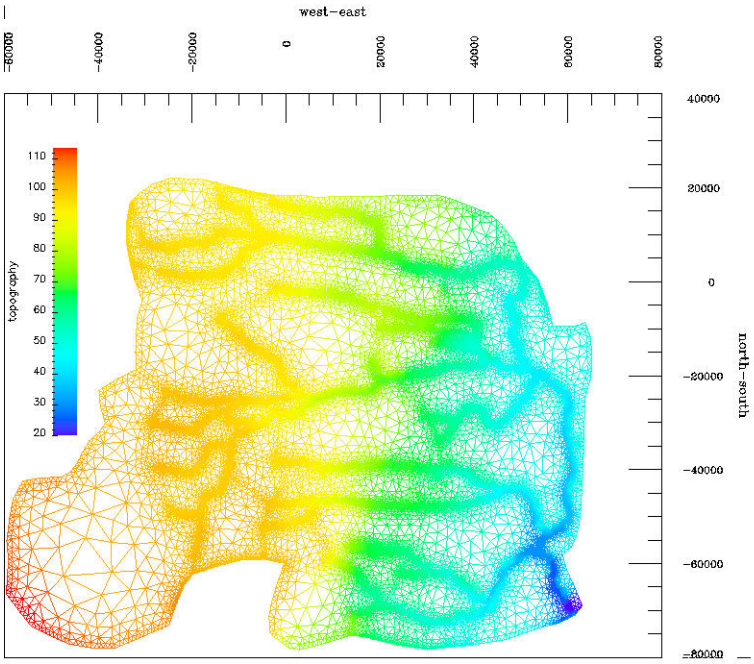

Figure 8: Aquifer/Stream mesh over topography.

4 FEM COMPUTATIONS.

The large time and length scales present in surface-water and ground-water flow problems entails to a large demand of computational resources. Typically, the range of length scales vary between hundred of kilometers and hundred of meters while time scale vary between days and years. A rough estimation suggests that triangulations, in the order of 100,000 to 1,000,000 triangles, should be used. Moreover, considering multi-aquifer system with several layers, the number of unknowns will be 10 to 20 unknowns per node. Therefore, the expected number of unknowns lies between 10^6 and 10^7.

Regarding the efficiency of parallelism, FEM computations can be split basically in two parts, a) matrix and right-hand side assembly and b) linear system solution. The right hand-side and the matrix can be assembled in each processor almost independently, with the exception of the contribution of nodes in the inter-subdomain interfaces. This requires some inter-processor communication, but this is usually irrelevant, specially for very large problems (In fact, the relation communication/computation for the assembly stage and for a given fixed problem scales with h, the mesh size.) The solution stage requires more communication and, then, is less parallelizable. The strategy used in this work is to use a Domain Decomposition Method, i.e. a mixture of iterative and direct solvers. We iterate a GMRES method on the interface,[5–7] and solve with a LU factorization in the sub-domain interiors. With this strategy, high computational efficiency can be attained. We adopt the trapezoidal rule for time integration.

5 NUMERICAL RESULTS.

We present two examples of surface and subsurface interaction flow for the Cululú basin. The cases have periodic rainfall. Different species with different evapotranspiration have been planted. The first case is a random soybean plantation (50 % of total area and an evapotranspiration 50% less than eucalyptus plantation), (see Fig. 9). In the second case only eucalyptus are planted.We simulate a year where the total precipitation is the annual average precipitation observed in last years (1,000 mm/year), but divided in two wet seasons with a rainfall rate of 2000 mm/year (april-march and september-october) and dry seasons of 500 mm/year (the rest of the year).
At time $t = 0$ the piezometric height in the freatic aquifer is 30 meters above the aquifer bottom, while the water height in stream is 10 meters above the streambed. The hydraulic conductivity and storativity of freatic aquifer are $2 \cdot 10^{-3} \frac{m}{sec}$ and $2.5 \cdot 10^{-2}$, respectively. We adopt the Manning friction law. The roughness of stream channel is $3 \cdot 10^{-3}$ and the river width is 10 meters. The *stream loss* resistivity average value is $10^5 sec$. A mesh of 96,131 triangular elements and 48,452 nodal points is used to represent the aquifer domain (see Fig. 8). The average space between nodal river points is 100 meters. The time step adopted in both cases is $Dt = 1$ day. In Fig. 10 we can see the correlation

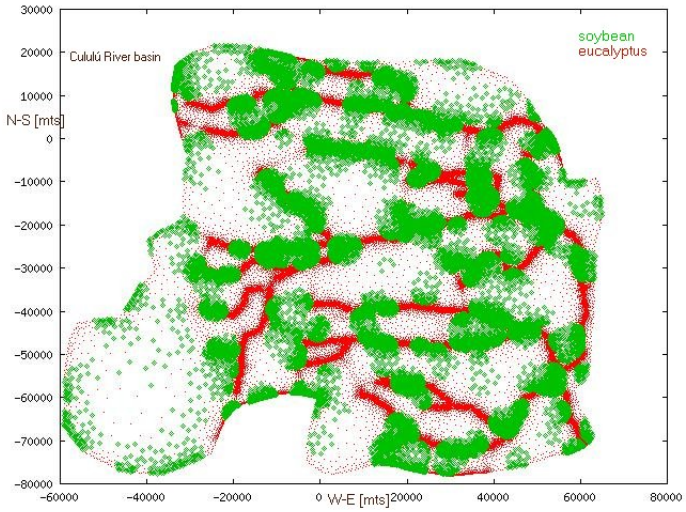

Figure 9: Soybean location.

between the presence of soybean and a greater freatic elevation with respect to the levels observed in the case where only eucalyptus are present. In Fig. 11 we can see the freatic elevation after two years of simulation. The time used to solve each time step in the nonlinear coupled problem with 6 processor Pentium IV 1.4-1.7 Ghz and 512 Mb RAM (Rambus) connected through a switch Fast Ethernet (100 Mbit/sec, latency=$O(100)$) was 13.2 seconds in average.

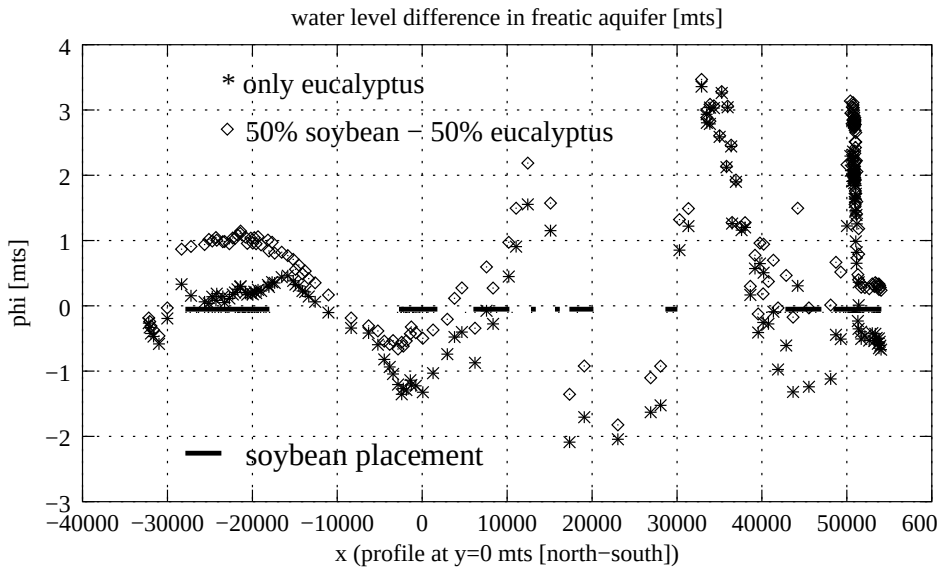

Figure 10: Difference in freatic levels for both cases.

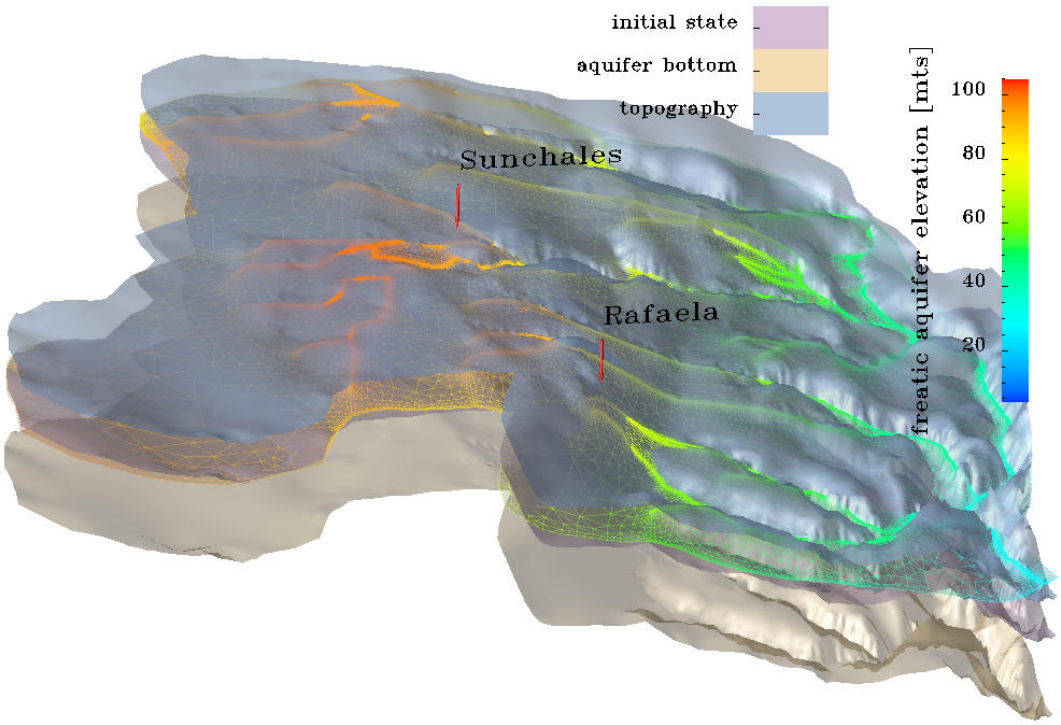

Figure 11: Aquifer State at t=2 years.

6 CONCLUSIONS.

The goal of the present work was the development of a large scale hydrological model for surface and subsurface water flow running in a cluster of PC's and the posibility of choosing among different models for the surface flow and also the suitable treatment of the different boundary conditions that arise in hydrology. More accurate physical data being obtained through intensive measurements work. Future work includes multi-layers/multi-aquifer systems, pollutant transport, etc.

ACKNOWLEDGMENT.

This work has received financial support from *Consejo Nacional de Investigaciones Científicas y Técnicas* (CONICET, Argentina), *Agencia Nacional de Promoción Científica y Tecnológica* (ANPCyT) and *Universidad Nacional del Litoral* (UNL) through grants CONICET PIP 198/ *Germen-CFD*, ANPCyT-PID-99/74 *FLAGS*, SECyT-FONCyT-PICT-6973 *PROA* and CAI+D-UNL-PIP-02552-2000. We made extensive use of freely distributed software as *GNU/Linux* OS, MPI, PETSc, Newmat, Metis, Octave, the CGAL geometrical library, OpenDX and many others.

REFERENCES

[1] L. B. Rodríguez. *Investigation of Stream-Aquifer Interactions Using Coupled Surface-Water and Ground-Gater Flow Model. Phd. Thesis*. University of Arizona, (1995).

[2] R. R. Paz, M. A. Storti, S. R. Idelsohn, L. B. Rodríguez, C. Vionnet, and G. Farias. Parallel finite element model for surface and subsurface hydrology. In *First South-American Congress on Computational Mechanics - III Brazilian Congress on Computational Mechanics - VII Argentine Congress on Computational Mechanics*, (2002).

[3] INRIA Sophia Antipolis and community of researchers. *The CGAL Basic Library.* INRIA, (2002).

[4] N. Sukumar. *The Natural Element Method in Solid Mechanics. Phd. Thesis.* Northwestern University, Illinois, (1998).

[5] M. A. Storti, L. Dalcin, R. R. Paz, V. Sonzogni, and A. Yommi. An interface strip preconditioner for domain decomposition methods. In *First South-American Congress on Computational Mechanics - III Brazilian Congress on Computational Mechanics - VII Argentine Congress on Computational Mechanics*, (2002).

[6] C. Farhat and F.X. Roux. A method of finite element tearing and interconnecting and its parallel solution algorithm. *Int. J. Numer. Meth. Eng.*, **32**, 1205–1227 (1991).

[7] P. Le Tallec and M. Vidrascu. Solving large scale structural problems on parallel computers using domain decomposition techniques. In M. Papadrakakis, editor, *Parallel Solution Methods in Computational Mechanics*, chapter 2, pages 49–85. John Wiley & Sons Ltd., (1997).

[8] R. Sibson. A brief description of natural neighbour interpolation. In V. Barnett, editor, *Interpreting Multivariate Data*, pages 21–36. John Wiley & Sons Ltd., (1981).